Anisotropic Ambiguities in TI Media

Ian F. Jones
Mike L. Bridson
&
Nick Bernitsas

Ian F. Jones (corresponding author)
GX Technology
180 High Street, Egham
Surrey TW20 9DN
Tel: +44 1784 497630
Email: ijones@gxt.com

Anisotropic Ambiguities in TI media

Ian F. Jones[1], Mike L. Bridson[1], & Nick Bernitsas[2]
1: GX Technology, 180 High Street, Egham, Surrey TW20 9DN, UK
2: GXT Corporation, 2101 CityWest Blvd. Building III, Suite 900, Houston, TX 77042, USA.

Introduction

In recent years we have seen processing and imaging algorithms re-written to handle anisotropic effects. The most common type of anisotropy that one deals with in seismic data is polar anisotropy (transverse isotropy). Media with vertical (VTI), tilted (TTI), and horizontal (HTI) axes have been shown to exist as a result of sedimentary deposition or fracturing.

The consequences of ignoring polar anisotropy vary depending on the degree and type of anisotropy. Typically, using isotropic imaging in an anisotropic medium results in mis-ties between the preSDM and the well depths. Such mis-ties, in some extreme cases, can exceed 10% of the true depth (for example, in the Franklin-Elgin field operated by TFE in the North Sea there is a 600m mis-tie at a depth of 5km). In addition to the vertical depth error, there is also a lateral shift, most pronounced for the steepest dips, and noticeable in fault surface reflections. Experience has shown that one cannot image simultaneously flat and steep dips with an isotropic velocity field.

The difficulty in addressing anisotropy lies in the estimation of reliable parameters to be used with the processing or imaging algorithms. In this work, we assess the effects of errors in anisotropic parameter estimation for the case of polar anisotropy, and attempt to quantify the consequences of these errors with some specific synthetic examples.

Background to Anisotropic Terminology

There are three classes of true anisotropy, some with sub-classes:

1. Intrinsic or inherent anisotropy (with 4 sub-classes)
   a) Crystalline anisotropy (with 7 crystal groups)
   b) Constraint induced (e.g. when micro-fissures are held open or closed by lithological confining pressure).
   c) Lithologically induced (e.g. polar anisotropy due to preferential sedimentary deposition of plate-like grains, or to plate-like crystal formation during metamorphosis)
   d) Paleomagnetically induced (during sedimentation, magnetic minerals will settle with a preferential direction. This may give rise to a detectable seismic anisotropy)

2. Crack induced anisotropy
This type of anisotropy is governed by large scale fractures which readily manifest themselves with a seismic response (this has a different form from the micro fractures which are controlled by confining pressure)

3. Long wavelength anisotropy (with 2 sub-classes)
This is a compound effect created by placing many adjacent regions next together: each region itself may be isotropic, but the net effect creates a form of anisotropy. There are two sub-classes here:
   a) Periodic thin layered
   b) Checkerboard

Due to symmetries, the 81 components of the elastic compliance tensor reduce to 21 for the most general anisotropic medium; further reductions are achieved for simpler media. For example, a TI medium can be described by only 5 coefficients plus the density. Approximations introduced for the case of weak transversely isotropic media have further simplified the complexity of the problem so that only one additional parameter is required for time imaging, and two additional parameters for depth imaging.

The most common formulations of these parameters are those described by Thomsen (1984), and those described by Alkhalifah & Tsvankin (1995). For time domain data, we can assess the degree of residual curvature on the far traces with the Alkhalifah eta (η) parameter, and for depth imaging, we can describe the depth discrepancy and residual far offset moveout with Thomsen's delta and epsilon (δ & ε) parameters (respectively).

The delta parameter is most easily obtained from the depth mis-match between a well and the depth migrated seismic image, and the epsilon parameter either from far offset residual moveout analysis, or from tomographic inversion.

Polar Anisotropy

The term anisotropy implies changes in sound speed as a function of propagation direction. For example, if energy propagates vertically, it moves with a different speed than if it propagates horizontally at the same point in a medium. In general, for media that are

layered, such as interbedded sands and shales, or media that have plate-like mineral grains, sound waves propagate more slowly perpendicular to the layers (or grains) than they do parallel to the layers (or grains).

For a horizontally layered anisotropic earth, the sound speed measured in a vertical well will be slower than that measured from surface seismic data. This is because the surface seismic data samples many angles of propagation due to the long offsets recorded in the data. Typically, vertical well velocities will be up to 10% lower than the corresponding surface seismic velocities (although for a small percentage of rocks, the well velocities can be higher, due to the interplay between pore and overburden pressure). The measured seismic velocity is neither the vertical velocity nor the horizontal velocity, but some hyperbolic move-out fit to a mix of both (Levin, 1978, Al-Chalabi 1974).

Consequently, whereas in an isotropic constant velocity medium, a wavefront propagates as a hemisphere, in an anisotropic medium, this shape will be flattened in the vertical direction, as the wavefront is expanding more rapidly laterally.

A commonly described form of anisotropy is the 'transversely isotropic' case. Here, the velocity is constant on the surface of a cone about some axis. If this axis of symmetry is vertical (VTI) then the velocity is azimuthally invariant (see figure 1). When the axis of symmetry is tilted, the medium is referred to as TTI. These forms of anisotropy are also referred to as polar or uni-axial.

Given a good velocity depth model of the subsurface, 3D depth migration will produce a reasonable 'geophysically' positioned image of the earth. This geophysical image may not correspond to true geological depth, unless such effects as anisotropy are taken into account. If we have been unable to handle the effects of anisotropy during migration, conversion from geophysical depth to geological depth can be achieved using various post-migration 'depthing' processes. However, a lateral mispositioning component will be present in a depth-converted isotropic image of anisotropic data.

Higher order (or 4th order) moveout:
For the multi-layer case mentioned above, we note that the moveout is characterized by a series expansion.

Figure 1: Symmetry axis in a VTI medium
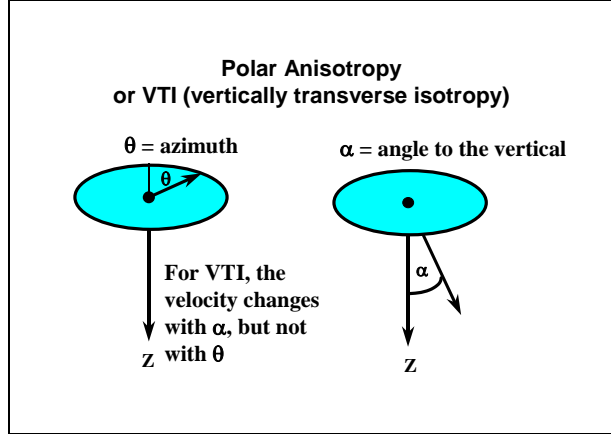
For moderate offsets (offset ~ depth) we can truncate this expansion to the second-order terms, and proceed with the assertion that the RMS velocity can be approximated by the NMO velocity, and that Dix inversion of these quantities will yield an interval velocity estimate. However, for longer offsets, this second-order expansion is inadequate, and several alternative expansions have been suggested (e.g. Al-Chalabi 1974, Hake et al 1984, Castle 1994). In the presence of vertical compaction gradients, the moveout corrections are even more complicated.

In general, for the isotropic flat multi-layered medium, the first three terms of the moveout expansion can be written as:

$$T_x^2 = T_o^2 + \frac{x^2}{V_{rms}^2} - \frac{x^4}{4T_o^2 V_{rms}^4}\left(\frac{\sum_j v_j^4 t_{oj}^2}{T_o^2 V_{rms}^4} - 1\right)$$

where: $\quad V_{rms}^2 = \dfrac{\sum_j v_j^2 t_{oj}}{\sum_j t_{oj}}$

v_j is the vertical interval velocity, and t_{0j} is the two-way vertical time in the jth layer.

Simply truncating the moveout expansion to the fourth order in x is a reasonable approximation to the reflection arrival times, but a better form can be used (e.g. Hake et al, 1984, Alkhalifah, 1997):

$$T_x^2 = T_o^2 + \frac{x^2}{V_{nmo}^2} - \frac{2x^4\eta}{V_{nmo}^2\left(T_o^2 V_{nmo}^2 + x^2(1+2\eta)\right)}$$

Here V_{nmo} is the short offset moveout velocity and eta (η) is a coefficient that describes aggregate ray bending effects. The first two terms of this expansion constitute the usual NMO equation.

Anisotropic large offset moveout effects, to a large extent, "mimic" those introduced by stacking a large number of isotropic layers, and it is often difficult to distinguish between the two from surface seismic data. For a VTI medium, a parameter eta (η) similar to that used for the isotropic case (see above) is needed to describe the moveout equation in the context of prestack time migration. For depth processing, two additional parameters, epsilon & delta (ϵ & δ) are required: these were characterised by Thomsen (1986).

In Thomson's notation, the vertical and horizontal velocities are related to the surface seismic near-offset moveout velocity (V_{nmo}) by:

$$V_{nmo} = V_v\,(1+2\delta)^{1/2}$$
$$V_h = V_v\,(1+2\epsilon)^{1/2}$$

Where:
  V_{nmo} is the near offset velocity estimated from stacking velocity analysis,
  V_v is the vertical velocity seen in well logs, and
  V_h is the horizontal component of velocity (which we do not usually have access to).

Alkhalifah's η parameter can be related to Thomsen's ϵ and δ formulation via:

$$\eta = (\epsilon - \delta)/(1+2\delta).$$

The relationship between V_{nmo} and V_v from Thomsen, is further simplified for small values of δ:

$$V_{nmo} \approx V_v\,(1+\delta).$$

In fact, for non-vertical propagation angles (as is the case for far offset analysis), this formulation is more appropriate (J.P. Jeannot, pers. comm.).

Alkhalifah (95, 97) described a cumulative effective anisotropy, which incorporates various non-hyperbolic moveout effects:

$$\eta_{eff}(T_o) = \frac{1}{8}\left\{\frac{\sum_j t_j v_j^4\left(1+8\eta_j\right)}{T_0 V_{nmo}^4} - 1\right\}$$

where v_j is the interval velocity derived from short-offset NMO velocities V_{nmo} using a Dix inversion.

For many rocks, velocity increases with depth of burial due to compaction of the sediments. This results in a moveout behavior similar to that of anisotropic media. As a consequence, the compaction gradient k, contributes to the overall measured (effective) anisotropy, and can be quantified by:

$$\eta_{eff} = \frac{1}{8}\left\{\frac{\left(0.5kT_0\right)}{\tanh\left(0.5kT_0\right)} - 1\right\}.$$

The cumulative effective anisotropy, η_{eff} can be measured from NMO'd data via:

$$\eta_{eff} = \frac{\Delta t^2 V_{nmo}^2\left(T_o^2 V_{nmo}^2 + X^2\right)}{2X^2\left(X^2 - \Delta t^2 V_{nmo}^2\right)},$$

Where: $\Delta t^2 = (T_O^2 - T_X^2)$.

Vertical Compaction Gradients and Anisotropy
First we look at synthetic gathers and velocity analysis panels for data created with anisotropy (ϵ=16%, δ=8%, Figures 2-4) and compare it with a gather containing only vertical compaction gradients (Figure 6). Figures 2-4 demonstrate the behavior of synthetic anisotropic data after moveout correction to 2nd and 4th orders. Note that 2nd order correction cannot flatten the gather and that η_{eff} measured from the data succeeds in doing so. Figures 5 is a schematic showing the effect of ray bending in a medium with a vertical compaction gradient. Figure 6 shows an isotropic synthetic CMP incorporating vertical velocity gradients after 2nd order NMO. Note that the far offset moveout behavior mimics that of the anisotropic case (Figure 2).

Synthetic Example
To assess the effect of ignoring vertical compaction gradients on anisotropic parameter estimation errors, we built a model based on a real North Sea case study, wherein we had an anisotropic package of sediments between the Balder and the BCU (Base Cretaceous Unconformity), and vertical compaction gradients in most layers (see Figure 7). We generated synthetic CMP data by ray-tracing in GXII, for a maximum offset of 6km, with CMP interval of 12.5m and 40 fold data. Figure 8 shows sample CMP's after NMO.

Figure 2: anisotropic CMP gather after 2nd order NMO correction using near vertical velocities. η_{eff} measured using Δt^2 at both 5km & 6km offsets, showing variation in η_{eff} due to picking uncertainty
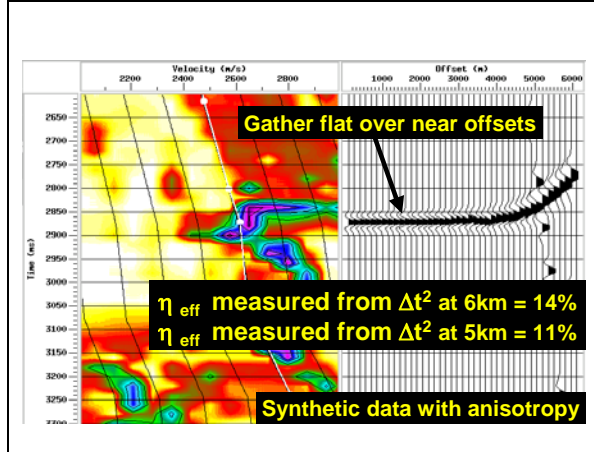

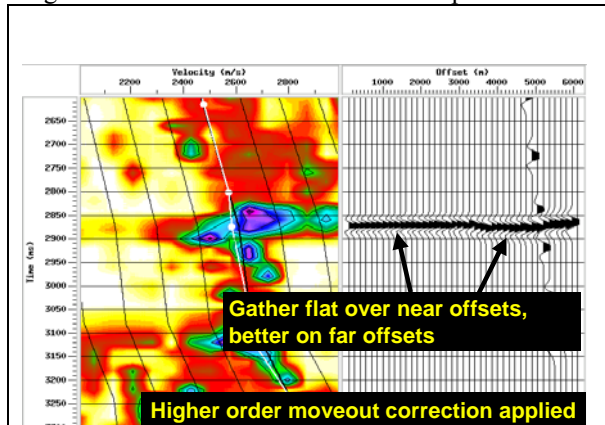Figure 3: 4th order correction of anisotropic CMP

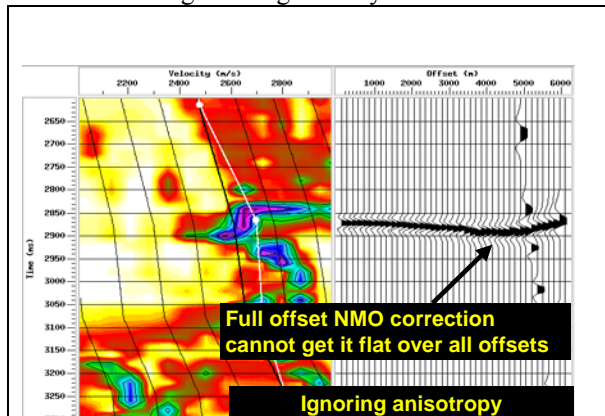Figure 4: anisotropic CMP after 2nd order NMO correction using stacking velocity derived over all offsets
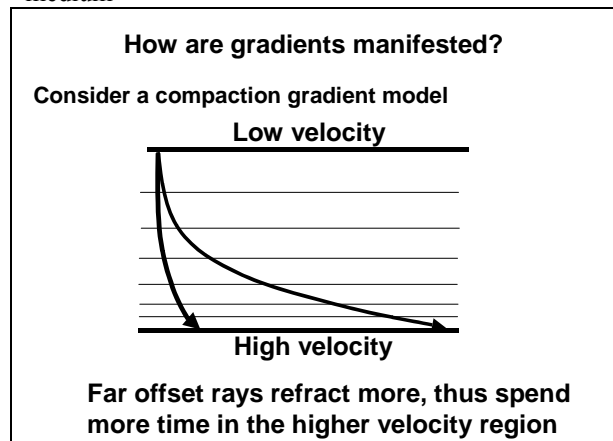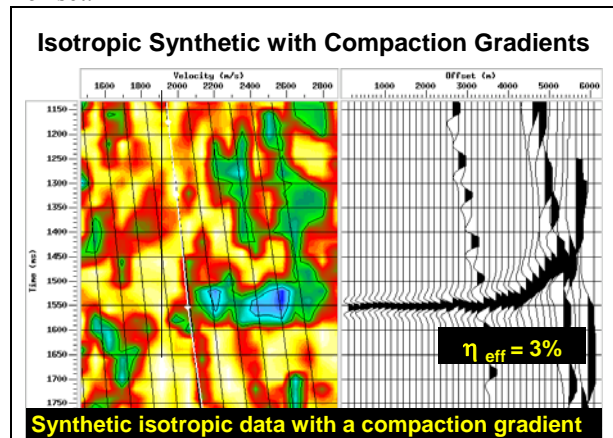

Figure 5: ray paths in vertical compaction gradient medium

Figure 6: Isotropic CMP for medium with vertical compaction gradient, after 2nd order NMO with near vertical velocities, η_{eff} measured using Δt^2 at 5km offset.

Using the 2nd order (near-vertical offset) V_{nmo} and the 4th order η_{eff} automatically picked estimates, we can flatten the gathers for the unmigrated input data (figure 9). For good quality clean data, this can yield good parameter estimates for the time processing parameter η_{eff}. However, for complex noisy real data, in general it can be easier to estimate parameters after migration.

These synthetic data were then subjected to a depth migration velocity model building procedure wherein the anisotropic parameters were estimated from a combination of measurements compared to wells (for the δ) and then automated 4th order moveout estimation followed by tomographic inversion to recover ε (assuming a fixed δ).

In the first model building exercise, we ignored the presence of vertical compaction gradients, but in the second exercise these gradients were included. The first case emulates the situation where we may only have access to tops to help with estimation of δ, but not the actual wells (thus gradients cannot be readily determined). Use of gradients in the second case emulates the situation were the wells are provided, and gradients measured.

In the preSDM results, we see a number of groups of migrated CRP gathers. All these results are plotted converted back to time for comparison. In figure 10 we have results for migrations ignoring vertical compaction, k. From left to right we have: gathers for isotropic migration; migration incorporating a δ value of 9% (as measured by comparing the isotropic migration and well-tops); a 4th order correction applied to the δ=9% CRPs using the η_{eff} values shown on the right. This is a QC plot to verify that the continuous autotracked η_{eff} values are reasonable. These η_{eff} values are estimated from the results of the δ=9% preSDM.

From the measured η_{eff} values (~15% at 2.9s), we invert for ε, and re-migrate the data. Figure 11 shows the results (third panel) compared to the 'correct' result (migrated using the known model), and also to the isotropic and δ=9% preSDM's. The values of ε obtained from η_{eff} inversion, after ignoring k, are over-estimated (ε ~23% at 2.9s), and the migration is not good.

In figures 12 & 13, these comparisons are repeated but this time incorporating the vertical compaction gradients k, during preSDM. The model building now almost perfectly recovers the anisotropy parameters (δ=8% & ε=15%, compared to the true values of δ=8% & ε =16%).

Figure 14 shows a summary of the seven migrations for a single CRP gather, plotted in depth. In addition to the visible vertical error in those migrations that exclude δ, we have noted the corresponding lateral mispositioning (measured on a pinch-out event at the base of the anisotropic layer, as indicated by the arrow in Figure 7).

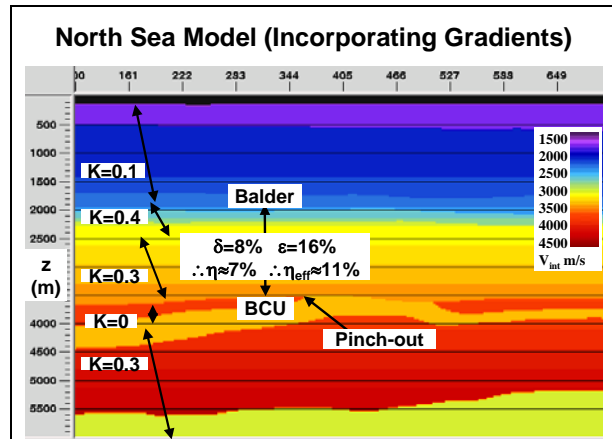Figure 7:interval velocities, ε, δ, & k values for a North Sea model

Figure 8: selected CMP gathers after near vertical NMO. No mutes are used, so as to preserve far-offset effects (consequently, some NMO stretch effects remain visible on the far-offsets)
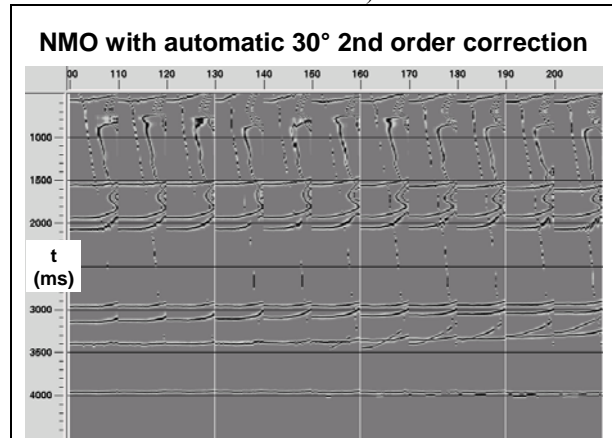

Figure 9: dense automatic η_{eff} scan (colour) and QC plot showing 4th order corrections
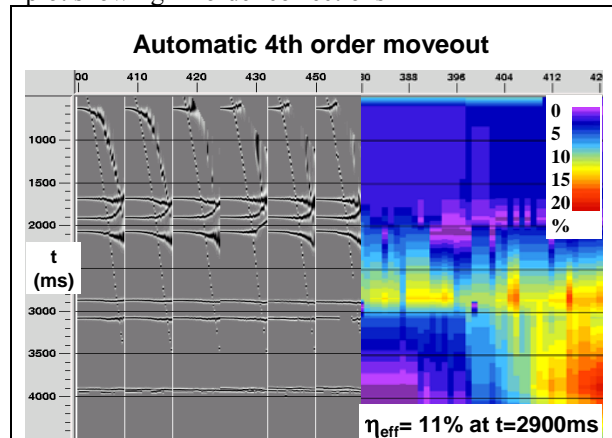
Figure 10: results of preSDM's ignoring compaction, and QC plot of 4th order moveout using estimated η_{eff} values
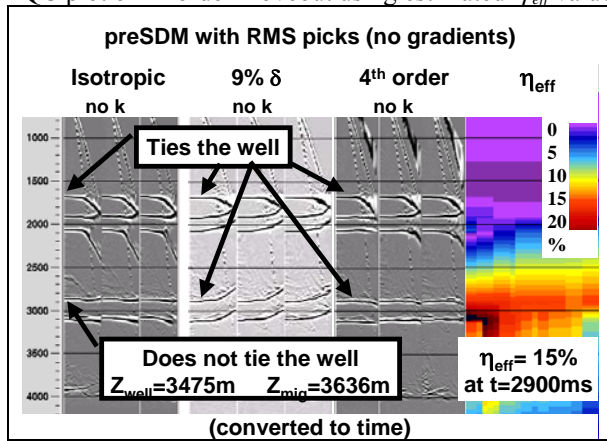

Figure 11: results of preSDM's (ignoring gradients) after inversion from η_{eff} to ε. Shown on the right is the correct result.
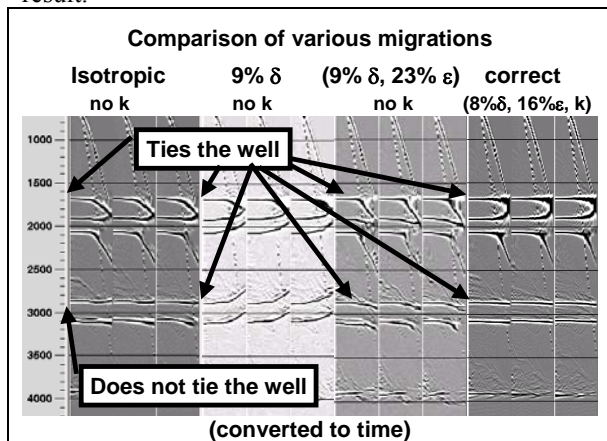

Figure 12: results of preSDM's including compaction, and QC plot of 4th order moveout using estimated η_{eff} values
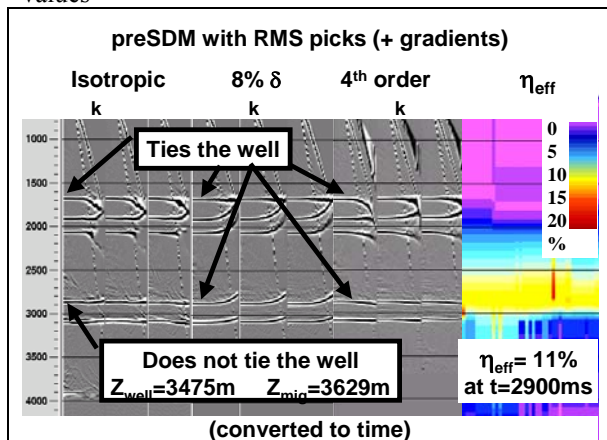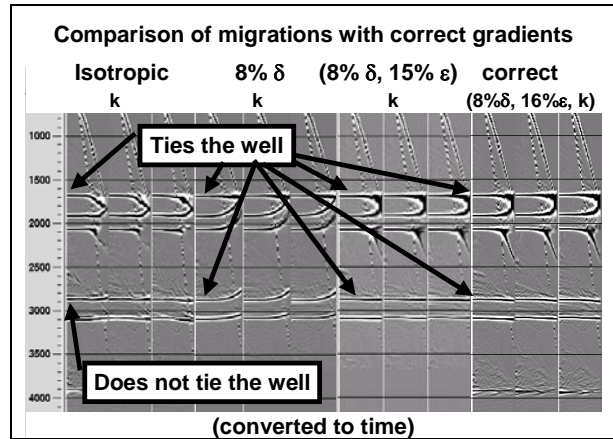

Figure 13: results of preSDM's (including gradients) after inversion from η_{eff} to ε. Shown on the right is the correct result.

Figure 14: comparison (in depth) of the 7 preSDM results, indicating measured lateral positioning errors.
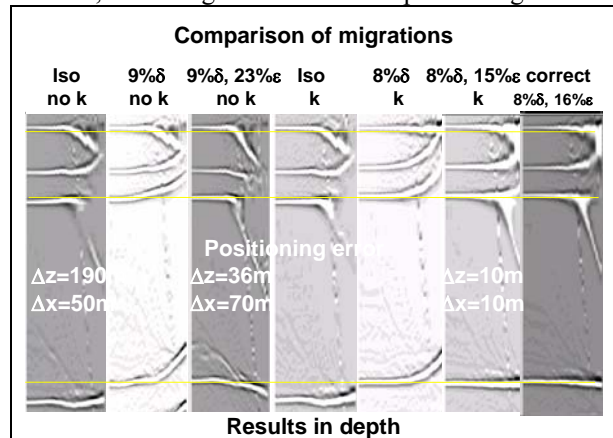

North Sea Example

The seismic data example shown here comes from an area with a thick anisotropic shale overburden, and targets below the BCU (Base Cretaceous Unconformity). In Figure 15, we see a CRP gather resulting from three different runs of 3D preSDM. In the first, we have an isotropic migration, where the velocity model was built so as to flatten the CRP gather. In the second, we have the result from an anisotropic migration with δ estimated from well mis-ties. In the third result, we have estimated ε from the far-offset residual moveout.

In this case, it is clear that we can improve on isotropic imaging in as much as we tie the well, and preserve the quality of fault imaging after the anisotropic migration. In figure 16 & 17, we see the improved fault imaging

after anisotropic migration. In addition, a 180m well mistie was resolved. These images are converted back to time.
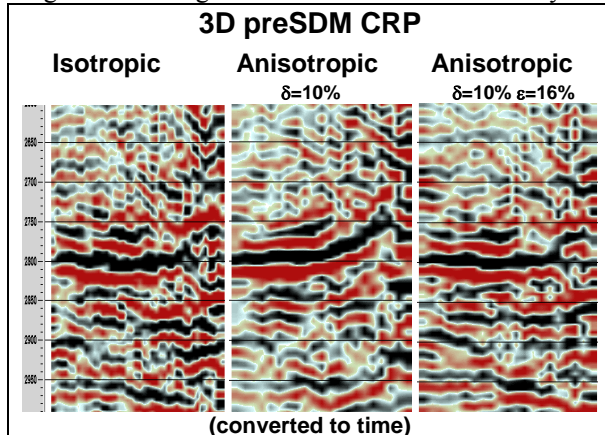
Figure 15: CRP gathers from North Sea case study.

(converted to time)

Figure 16: faulted tilted target below unconformity

(converted to time)
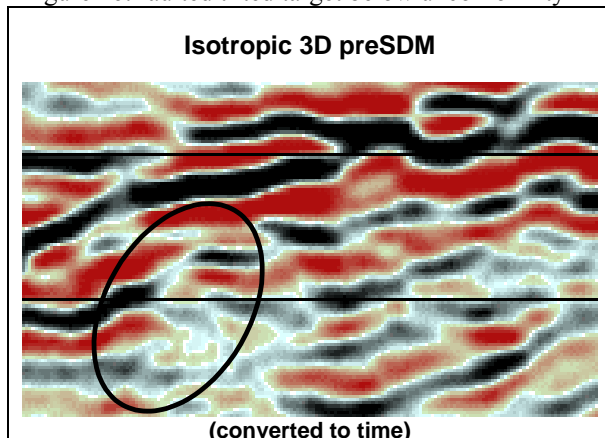
Figure 17: improved fault imaging, and well tie

(converted to time)
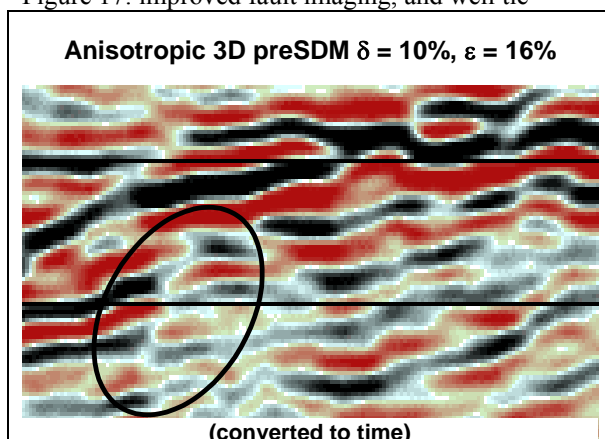
Depthing versus Migration

The question does arise as to whether it is 'safer' to migrate isotropically, and then convert to geological depth (calibrated to the wells) *after* the depth migration. In this case, we would have the trade-off between simplicity in the model building versus potential lateral positioning errors.

An example of this is shown in figures 18 & 19. Here we have generated synthetic anisotropic data, and have then migrated it with two different models. The first was a model derived from the data using tomographic inversion but ignoring the anisotropy. The second is the correct model, including anisotropy, used to generate the data.

After the migrations, the images have been converted to time with their respective models. In this instance, we see that the error committed by ignoring anisotropy has not significantly degraded the image, nor induced much lateral positioning error in this particular case. This is not a general conclusion, but for modest anisotropy, 'depthing' following an isotropic migration is an option.

The safest way to assess this problem is simply to create a synthetic 2D anisotropic data set, migrate it both anisotropically and isotropically, and then assess the relative errors after conversion back to time with their respective models.

Conclusions

Anisotropic time and depth migration are now well established approaches to imaging in complex areas, and including the effects of anisotropy can result in sharper images that correctly tie the wells. However, it must be recognized that anisotropic effects can be masked by, or confused with other phenomena.

Although a reasonable depth-tied image can be obtained with non-physical parameters, we must be aware of this limitation when using the anisotropic parameters for petrophysical studies. The 'anisotropy' we measure can be a compound effect incorporating several phenomena
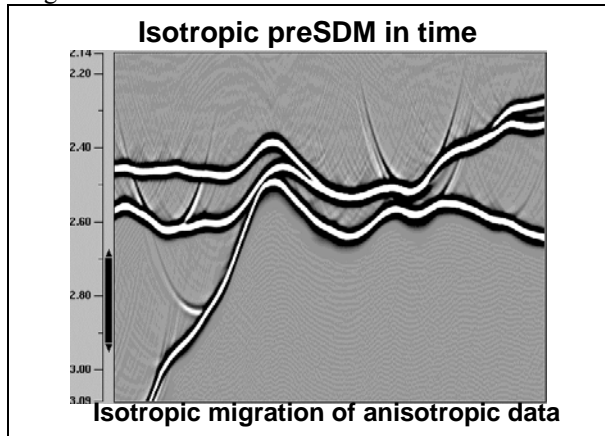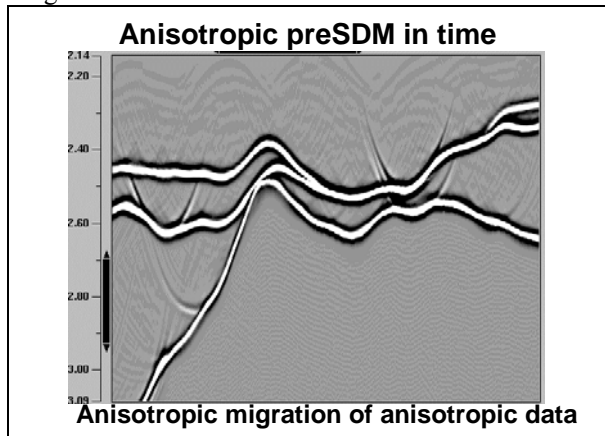
Figure 18

Isotropic preSDM in time

Isotropic migration of anisotropic data

Figure 19

Anisotropic preSDM in time

Anisotropic migration of anisotropic data

References
Al-Chalabi, M., 1974, an analysis of stacking, rms, average, and interval velocities of horizontally layered ground. Geophys. Prosp., 22, 458-475.

Alkhalifah, T., & Tsvankin, I., 1995, Velocity analysis for transversely isotropic media; Geophysics, 60, no.5, 1550-1566.

Alkhalifah, T., 1997, Velocity analysis using nonhyperbolic moveout in transversely isotropic media; Geophysics, 62, no.6, 1839-1854.

Castle, R.J., 1994, A theory of normal moveout, Geophysics, 59, no.6, 983-999.

de Bazelaire, E., 1988, Normal move-out revisited: inhomogeneous media and curved interfaces, Geophysics 53, 143.

Hake, H.., Helbig, K., & Mesdag, C.S. 1984, Three-term Taylor series for t2-x2 curves over layered transversely isotropic ground, Geophys. Prosp., 32, 828-850.

Levin, F.K., 1978, The reflection, refraction, and diffraction of waves in media with elliptical velocity dependence: Geophysics, 43, 528.

Swan, H.W., 1991, Amplitude versus offset measurement errors in a finely layered medium. Geophysics, 56, no.1, 41-49.

Tatham, R.H., & McCormack, M.D, 1993, Multicomponent seismology in petroleum exploration; Investigations in Geophysics Series, v6, SEG.

Thomsen,L, 1986, Weak elastic anisotropy; Geophysics, 51, no.10, 1954-1966.

Tsvankin, I, and Thomsen, L., 1994, Nonhyperbolic reflection moveout in anisotropic media. Geophysics, 59, 1290-1304.